Journal of Magnetic Resonance **156,** 146–151 (2002)
doi:10.1006/jmre.2002.2545

Two-Dimensional High-Resolution NMR Spectra in Matched B_0 and B_1 Field Gradients

Henrike Heise, Dimitris Sakellariou, Carlos A. Meriles, Adam Moulé, and Alexander Pines[1]

Materials Sciences Division, Lawrence Berkeley National Laboratory and Department of Chemistry, University of California—Berkeley, Berkeley, California 94720

Received January 18, 2002; revised April 4, 2002

In a recent publication we presented a method to obtain highly resolved NMR spectra in the presence of an inhomogeneous B_0 field with the help of a matched RF gradient. If RF gradient pulses are combined with "ideal" 90° pulses to form inhomogeneous z rotation pulses, the line broadening caused by the B_0 gradient can be refocused, while the full chemical shift information is maintained. This approach is of potential use for NMR spectroscopy in an inhomogeneous magnetic field produced by an "ex-situ" surface spectrometer. In this contribution, we extend this method toward two-dimensional spectroscopy with high resolution in one or both dimensions. Line narrowing in the indirect dimension can be achieved by two types of nutation echoes, thus leading to depth-sensitive NMR spectra with full chemical shift information. If the nutation echo in the indirect dimension is combined with a stroboscopic acquisition using inhomogeneous z-rotation pulses, highly resolved two-dimensional correlation spectra can be obtained in matched field gradients. Finally, we demonstrate that an INEPT coherence transfer from proton to carbon spins is possible in inhomogeneous B_0 fields. Thus, it is possible to obtain one-dimensional ^{13}C NMR spectra with increased sensitivity and two-dimensional HETCOR spectra in the presence of B_0 gradients of 0.4 mT/cm. These schemes may be of some value for ex-situ NMR analysis of materials and biological systems.

Key Words: **nutation echo; magnetic field gradient; RF gradient; ex-situ NMR; 2D NMR.**

INTRODUCTION

The analytical information content of an NMR spectrum is related to the number of lines that can be distinguished for a given bandwidth and under given experimental conditions. Typically, the most useful spectral parameter is the chemical shift, so it is desirable to use a homogeneous external field in order to produce a high chemical shift resolution. However, for many applications, it would be convenient if a mobile magnet could be scanned over the surface of an otherwise unaccessible object or subject in order to obtain magnetic resonance information. Indeed, in the past decade, much effort has been put into the development of surface NMR spectrometers (*1, 2*) for applications like well logging (*3*), materials science (*4*), and biomedicine (*5*). The main drawback of such ex-situ NMR spectroscopy is the large inhomogeneity of the magnetic field produced by a surface scanner. The detection sensitivity can be enhanced by the use of Carr–Purcell echo trains (*3, 6*), which refocus not only the effect of the field inhomogeneity but also the chemical shift information. Therefore, the information content of ex-situ NMR spectroscopy has been limited to relaxation parameters (7) and multiquantum buildup curves (*8*) in order to discriminate between different material domains, whereas chemical shifts are typically not resolved in such "ex situ" spectrometers. Recently, a research group used matched gradients of the magnetic field and RF field in order to generate so-called nutation echoes and to apply them for localized NMR spectroscopy (*9, 10*).

In the past, various two-dimensional sequences for the elimination of line-broadening due to inhomogeneous magnetic fields have been developed (*11–16*) which are based on delayed acquisition (*17*) superimposed on coherence transfer echoes (*18*). Here, the indirect dimension yields highly resolved spectra, but it displays only the differences between the chemical shifts of the evolving coherences and the observed nuclei instead of the direct chemical shifts. The relative chemical shifts of the nuclei can therefore only be extracted directly if all nuclei are correlated to the same nucleus (*16*) or the the same multiquantum coherence (*14, 15*), conditions which are not easily fulfilled for most samples.

In a recent publication we presented an approach toward high resolution ex-situ NMR spectroscopy (*19*) that is based on nutation echoes (*9, 10, 20*) due to RF field gradients which are perpendicular to the static field B_0 and proportional to the static field gradient. For sample regions where the static field and the RF field (B_1) gradient are matched, or where the effective RF gradient can be matched to the static field by appropriate composite pulses, the line-broadening caused by B_0 inhomogeneities can be refocused during the acquisition period by applying a train of RF gradient pulses (see below). These B_1 gradient pulses do not refocus the evolution of the magnetization under the effect of intrinsic fields due to chemical shift and indirect couplings, and thus the full spectroscopic information is recovered. In this

[1] To whom correspondence should be addressed. Fax: (510) 486-5744. E-mail: pines@cchem.berkeley.edu.

1090-7807/02 $35.00

paper we extend this method toward depth sensitive NMR spectroscopy and highly resolved two-dimensional homo- and heteronuclear correlation spectroscopy using polarization transfer (INEPT).

THEORY

Nutation Echoes

If the gradients of the static magnetic field, $\mathbf{G}_0$, and the effective radiofrequency field, $\mathbf{G}_1$, are parallel and their magnitudes are proportional, such that $\mathbf{G}_1(r) = k \cdot \mathbf{G}_0(r)$ over a certain region of the sample, a nutation echo can be produced by a single radiofrequency pulse: The RF gradient pulse spreads the magnetization in the yz-plane. During the following time interval t the transverse component of the magnetization evolves under the influence of the magnetic field gradient $\Delta\omega_0(r)$, and the chemical shift, Ω.

$$\begin{aligned} I_z &\xrightarrow{(G_1)_x} I_z \cdot \cos(\omega_1(r)\tau) - I_y \cdot \sin(\omega_1(r)\tau) \\ &\xrightarrow{G_0,\Omega} I_z \cdot \cos(\omega_1(r)\tau) - I_y \cdot \sin(\omega_1(r)\tau) \cdot [\cos(\Delta\omega_0(r)t) \\ &\quad \cdot \cos(\Omega t) - \sin(\Delta\omega_0(r)t) \cdot \sin(\Omega t)] + I_x \cdot \sin(\omega_1(r)\tau) \\ &\quad \cdot [\sin(\Delta\omega_0(r)t) \cdot \cos(\Omega t) + \cos(\Delta\omega_0(r)t) \cdot \sin(\Omega t)] \quad [1] \end{aligned}$$

If $\omega_1(r) = \omega_1(0) + k \cdot \Delta\omega_0(r)$ for a given volume element of the sample, r, a nutation echo is formed after a time $t = k \cdot \tau$:

$$\begin{aligned} &I_z \cdot \cos\left(\Delta\omega_0 t + \omega_1(0)\frac{t}{k}\right) + 0.5 \cdot I_x \cdot \left[\cos\left(\Omega t - \omega_1(0)\frac{t}{k}\right)\right. \\ &\left. - \cos\left(2\Delta\omega_0(r)t + \Omega t + \omega_1(0)\frac{t}{k}\right)\right] \\ &+ 0.5 \cdot I_y \cdot \left[\sin\left(\Omega t - \omega_1(0)\frac{t}{k}\right)\right. \\ &\left. - \sin\left(2\Delta\omega_0(r)t + \Omega t + \omega_1(0)\frac{t}{k}\right)\right]. \quad [2] \end{aligned}$$

This nutation echo is related to the original Hahn echo (*21*) produced by two 90° pulses in an inhomogeneous magnetic field: At the beginning of the refocusing period, the magnetization is dephased in the xz-plane, and at the end of the refocusing period, half of the signal is recovered while the other half of the magnetization is dephased. However, assuming that the chemical shift evolution takes place only during the free evolution period and not during the RF pulse, this echo is, in contrast to the Hahn echo, modulated by the chemical shift, Ω, in addition to an overall modulation frequency $\omega_1(0)/k$.

The complete nutation echo can be recovered, if the inhomogeneous RF pulse is followed by an ideal 90° pulse, which is phase shifted by 90° with respect to the RF gradient pulse. This pulse brings the defocused magnetization from the yz-plane into the xy-plane before the full signal is refocused. This nutation echo is comparable to a Hahn echo produced by the sequence 90–τ–180–τ, but, again, it is modulated by the chemical shift, Ω, and an overall frequency modulation due to the RF-offset $\omega_1(0)/k$.

$$\begin{aligned} I_z &\xrightarrow{(G_1)_x} I_z \cdot \cos(\omega_1(r)\tau) - I_y \cdot \sin(\omega_1(r)\tau) \\ &\xrightarrow{90^\circ_y} I_x \cdot \cos(\omega_1(r)\tau) - I_y \cdot \sin(\omega_1(r)\tau) \\ &\xrightarrow{G_0,\Omega} I_x \cdot \{[\cos(\omega_1(r)\tau) \cdot \cos(\Delta\omega_0(r)t) + \sin(\omega_1(r)\tau) \\ &\quad \cdot \sin(\Delta\omega_0(r)t)] \cdot \cos(\Omega t) + [\sin(\omega_1(r)\tau) \cdot \cos(\Delta\omega_0(r)t) \\ &\quad - \cos(\omega_1(r)\tau) \cdot \sin(\Delta\omega_0(r)t)] \cdot \sin(\Omega t)\} \\ &\quad + I_y \cdot \{[\cos(\omega_1(r)\tau) \cdot \sin(\Delta\omega_0(r)t) - \sin(\omega_1(r)\tau) \\ &\quad \cdot \cos(\Delta\omega_0(r)t)] \cdot \cos(\Omega t) + [\cos(\omega_1(r)\tau) \\ &\quad \cdot \cos(\Delta\omega_0(r)t) + \sin(\omega_1(r)\tau) \cdot \sin(\Delta\omega_0(r)t)] \cdot \sin(\Omega t)\} \\ &\xrightarrow{t=k\cdot\tau} I_x \cdot \cos\left(\Omega t - \omega_1(0)\frac{t}{k}\right) + I_y \cdot \sin\left(\Omega t - \omega_1(0)\frac{t}{k}\right) \quad [3] \end{aligned}$$

This sequence yields a higher signal-to-noise ratio; however, it requires an ideal 90° pulse around the same rotation axis for all spins throughout the detected sample region, regardless of the RF field strength. Such 90° rotations can be implemented with constant rotation B_1 insensitive composite pulses.

Pulse Sequences

Based on the concept of nutation echoes in the indirect dimension, a very simple pulse sequence, yielding a depth sensitive 2D NMR spectrum with high resolution in the indirect dimension, is suggested in Fig. 1a. It consists of one single RF gradient pulse, the duration of which is incremented together with t_1 in such a way that the acquisiton begins at the peak of the echo. Note that this pulse sequence is similar to the well-known two-dimensional nutation experiment (*9, 22*) with a delayed acquisition (*17*); such a sequence is also used in order to probe the matching of the field gradients, if the acquisition starts immediately after the RF gradient pulse. Figure 1b displays a variation of this pulse sequence, which uses a constant rotation composite 90° pulse after the RF gradient and therefore leads to a recovery of the complete signal.

In Figs. 1c and 1d, two versions of stroboscopic refocusing pulse sequences are depicted. These sequences exploit full nutation echoes, induced by the composite z rotation pulses (90°_{-y}–$\beta(r)_x$–90°_y), where the 90° pulses are accomplished by constant rotation composite pulses. In each case, each point of the FID is acquired stroboscopically in synchronism with such a nutation echo (*19*), and a homogeneous spectrum with chemical shift information can be obtained in the direct dimension. If the refocusing in the indirect dimension is combined with a coherence transfer superimposed on the nutation echo and stroboscopic acquisition, a two-dimensional correlation spectrum can be obtained. If the coherence is transferred between nuclei

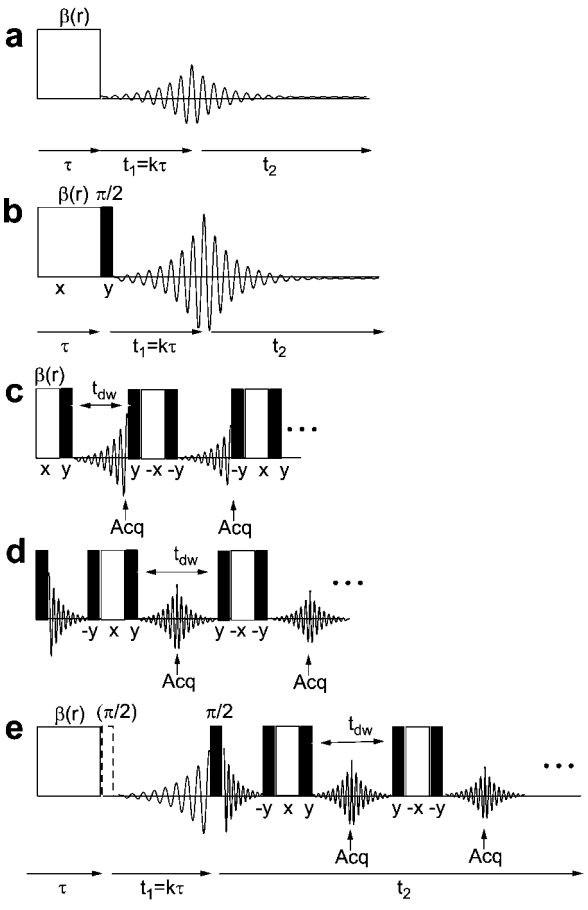

FIG. 1. Nutation echo based pulse sequences: ideal 90° pulses (approximated by constant rotation composite pulses; see text) are depicted in black, and inhomogeneous RF pulses are depicted in white. (a) 2D nutation echo sequence in the absence of a 90° pulse; (b) 2D nutation echo sequence with full signal recovery; (c) and (d) arrangements of inhomogeneous z-rotation composite pulses $(90^\circ_{-y})[\beta(r)_x](90^\circ_y)$ for stroboscopic acquisition of resolved spectra; (e) COSY pulse sequence with refocusing B_1 gradient pulses in both dimensions. The 90° pulse at the end of the inhomogeneous RF pulse in the indirect dimension is optional for signal enhancement.

of the same type, as in Fig. 1e, a refocused COSY spectrum is obtained, as described previously (*19*).

The refocusing sequences can be successfully extended to one- and two-dimensional ^{13}C NMR spectroscopy. In order to increase the sensitivity, direct acquisition of ^{13}C signals was combined with an INEPT transfer (*23*) from proton to carbon spins (Fig. 2a) with constant rotation composite 90° and 180° pulses on both channels. After the first excitation pulse on the protons, the density matrix contains pure antiphase coherence $2I_yS_z$ at the end of the time interval $1/2J$; chemical shift and B_0 inhomogeneities are refocused by the simultaneous 180° pulses on both nuclei in the middle of this interval. The coherence transfer from ^{1}H to ^{13}C is performed by applying one 90° pulse to the ^{1}H spins which transforms the antiphase coherence into longitudinal two-spin order $2I_zS_z$, an inhomogeneous RF pulse of length τ' on the carbon channel, which dephases the carbon magnetization in the yz-plane. The second 90° pulse brings the dephased antiphase magnetization $2I_zS_x \cdot \cos(\omega_1(r)\cdot\tau) - 2I_zS_y \cdot \cos(\omega_1(r)\cdot\tau)$ into the xy-plane. The dephasing in the yz-plane refocuses under the influence of the matched B_0 gradient such that a nutation echo according to Eq. [3] is formed at the end of the dwell time t_{dw}, provided that the duration of the inhomogeneous RF pulse is adjusted to t_{dw} such that $t_{dw} = k\cdot\tau'$, when the first point of the FID is acquired. Stroboscopic acquisition with a pulse train consisting of inhomogeneous RF pulses of duration τ placed between two composite 90° pulses yields an FID which is modulated by the chemical shifts and indirect couplings, as described previously for protons. As the density operator contains pure antiphase coherence at the beginning of the stroboscopic acquisition, the resulting spectrum yields antiphase multiplets that depend on the proton multiplicity (*23*).

If the INEPT transfer is combined with a ^{1}H nutation echo in the indirect dimension and followed by stroboscopic acquisition on ^{13}C, a ^{1}H, ^{13}C HETCOR spectrum (*24*) with high resolution in both dimensions can be obtained in the presence of matched B_1 and B_0 gradients. A detailed HETCOR sequence with heteronuclear decoupling in the indirect dimension is shown in Fig. 2b: At the center of the free evolution period t_1 a homogeneous 180° pulse on the carbon spins is applied in order to achieve heteronuclear decoupling in the indirect dimension. In the subsequent time delay, $1/(2J)$, during which the antiphase magnetization evolves, field inhomogeneities as well as chemical shift evolution are refocused by a synchronous 180° pulse on both channels. The coherence transfer is accomplished by a

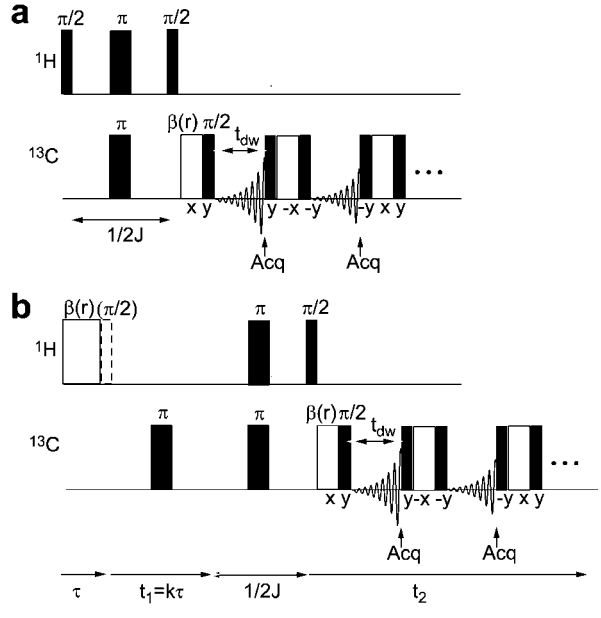

FIG. 2. Nutation echo based heteronuclear pulse sequences: "ideal" 90° pulses and 180° pulses are depicted in black, inhomogeneous RF pulses are depicted in white. (a) INEPT magnetization transfer step, followed by stroboscopic acquisition with a train of inhomogeneous z-rotation composite pulses $(90^\circ_{-y})[\beta(r)_x](90^\circ_y)$ on the ^{13}C-channel. (b) HETCOR pulse sequence yielding spectra with high resolution in both dimensions. The 90° pulse at the end of the inhomogeneous RF pulse in the indirect dimension is optional for signal enhancement.

homogeneous 90° pulse on the protons and one homogeneous 90° pulse on the carbon spins, preceded by an RF gradient pulse which defocuses the S magnetization in the yz-plane prior to the stroboscopic acquisition.

EXPERIMENTAL

All experiments were carried out in a Nalorac super-widebore imaging magnet using a Varian/Chemagnetics Infinity spectrometer operating at 179.12 and 45.042 MHz for ^{1}H and ^{13}C, respectively, and a home-built imaging probehead with three perpendicular gradient coils. A brief survey of the experimental setup is given in Ref. (*19*). In order to emulate ex-situ conditions inside the magnet bore, we produced a static field gradient by applying current to the x-gradient coils of the probehead. The sample was placed outside of the solenoidal RF coil, where a constant RF gradient prevails. An approximation to ideal 90° pulses was accomplished with the constant-rotation composite pulse $(2\gamma)_{97.2}(4\gamma)_{291.5}(2\gamma)_{97.2}(\gamma)_0$, whereas

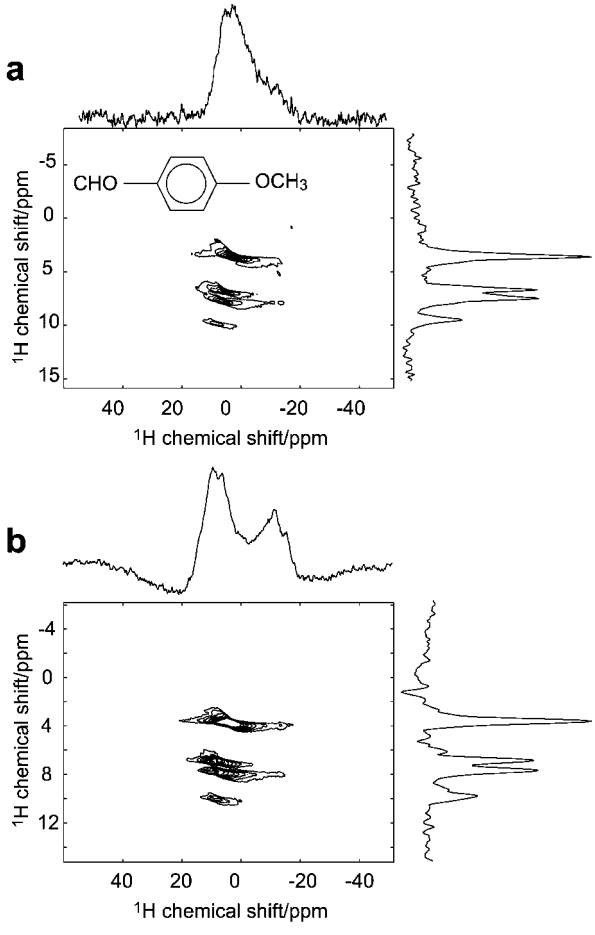

FIG. 3. Two-dimensional spectra of p-anisaldehyde in a magnetic field gradient of 0.25 mT/cm obtained using the pulse sequences displayed in Figs. 1a (a) and 1b (b). Both spectra were acquired with immediate detection after the pulse(s) and a shearing transformation corresponding to a ratio $k = t_1/\tau = 6.2$. The nominal 90° pulse length in (b) was 10 μs.

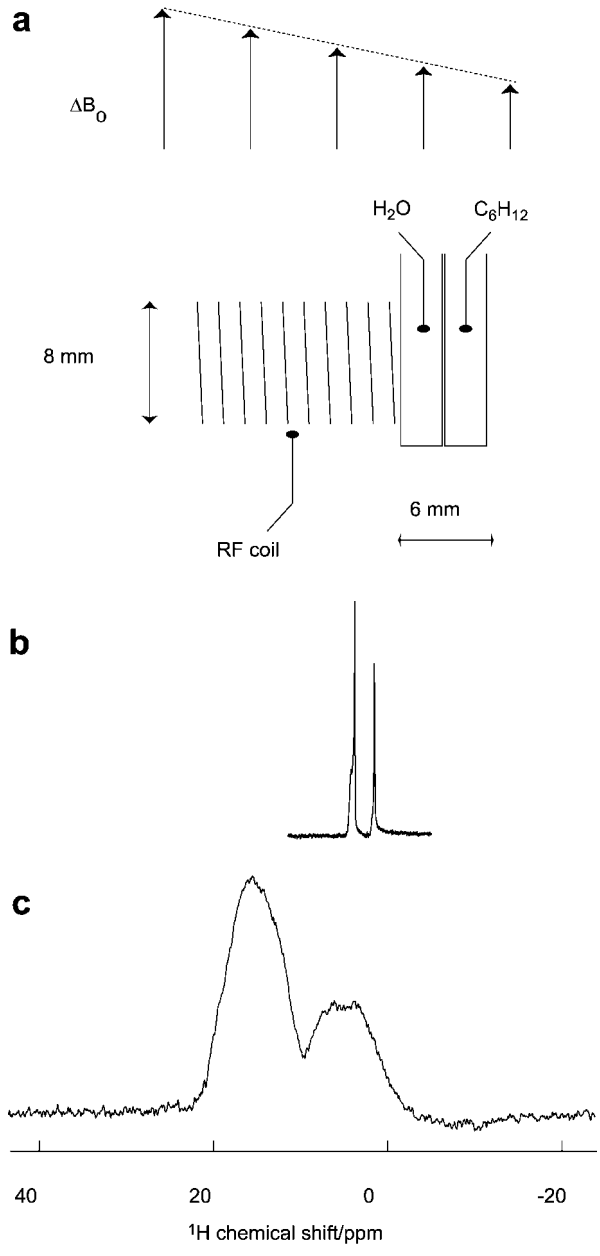

FIG. 4. (a) Sample setup with two tubes containing water and cyclohexane. (b) Homogeneous NMR spectrum obtained after one single pulse of length 14 μs. (c) Inhomogeneously broadened one-pulse spectrum in the presence of a constant gradient of 0.18 mT/cm.

that for 180° pulses was achieved by the composite pulses $(2\gamma)_{104.5}(4\gamma)_{313.4}(2\gamma)_{104.5}(2\gamma)_0$ (*25*).

Nominal 90° pulse lengths γ for the composite pulses were optimized to give the maximum signal intensity after one single RF pulse; typical 90° times ranged between 9 and 17 μs for both ^{13}C and ^{1}H. The lengths of the inhomogeneous β pulses for the stroboscopic acquisition were optimized to the narrowest linewidth for a given dwell time.

Depth-sensitive spectra were recorded with acquisition directly after the gradient pulses; a shearing transformation on

top of the echo was subsequently applied. The ratio between t_1 and τ, the length of the inhomogeneous RF pulse on the proton channel prior to t_1 in the HETCOR experiment was determined by recording a two-dimensional nutation spectrum according to pulse sequence 1a. In order to correct for the frequency offset $\omega_1(0)/k$, spectra were referenced to one signal with known chemical shift in the highly resolved dimension.

RESULTS AND DISCUSSION

Figure 3 displays two two-dimensional ^{1}H NMR spectra of *p*-anisaldehyde, obtained in a magnetic field of 4.2 T with a constant gradient of 0.25 mT/cm perpendicular to the field direction. The spectrum in Fig. 3a was obtained according to sequence 1a. The inhomogeneous RF pulse was followed immediately by acquisition; the t_1 delay was introduced subsequently by a shearing transformation of the two-dimensional data matrix before the Fourier transformation. In the indirect dimension four proton peaks in the ratio 3 : 2 : 2 : 1, corresponding to the methyl group, the two aromatic proton types, and the aldehyde proton, respectively, are clearly resolved. The indirect dimension shows the inhomogeneous line broadening due to the B_0 field inhomogeneity; the intensity of the signal is proportional to the receptivity of the RF coil. The spectrum in Fig. 3b was obtained with the same sample setup, under identical conditions, according to the pulse sequence of Fig. 1b. In the indirect dimension, the four signals are well resolved. The direct dimension displays a distortion which can be ascribed to the nonuniform excitation profile of the composite 90° pulse over the B_0 field.

In order to show its potential for use in spatially resolved NMR spectroscopy, pulse sequence 1a was applied to the sample setup displayed in Fig. 4a: Two sample tubes, one filled with water, the other one with cyclohexane, were placed next to each other outside the RF coil. The ^{1}H NMR spectrum in the absence of a B_0 gradient (Fig. 4b) displays two distinct peaks at 1.4 and 5.3 ppm for cyclohexane and water, respectively. In the presence of a B_0 gradient of 0.18 mT/cm, both peaks are broadened to a half width of 10 ppm and spatial encoding prevails over the chemical shift information (Fig. 4c). In Fig. 5, the two-dimensional spectrum, obtained with pulse sequence 1a, is shown. The spatial information in the direct dimension is correlated with the spectral information in the indirect dimension. Thus, a chemical shift image (*26*) in one dimension can be obtained under ex-situ conditions with such a simple approach.

The heteronuclear pulse sequences of Figs. 2a and 2b were tested with a sample of ethanol in a tube of 10-mm diameter,

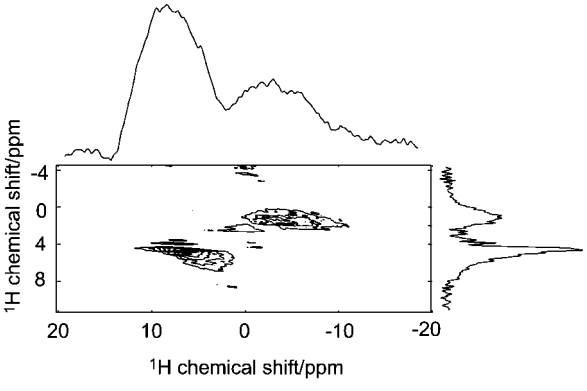

FIG. 5. Depth-sensitive ^{1}H NMR spectrum of the samples displayed in Fig. 4a, obtained with the pulse sequence of Fig. 1a in a field gradient of 0.18 mT/cm. The spectrum was acquired with immediate detection after the pulse and a shearing transformation corresponding to $k = t_1/\tau = 7.0$.

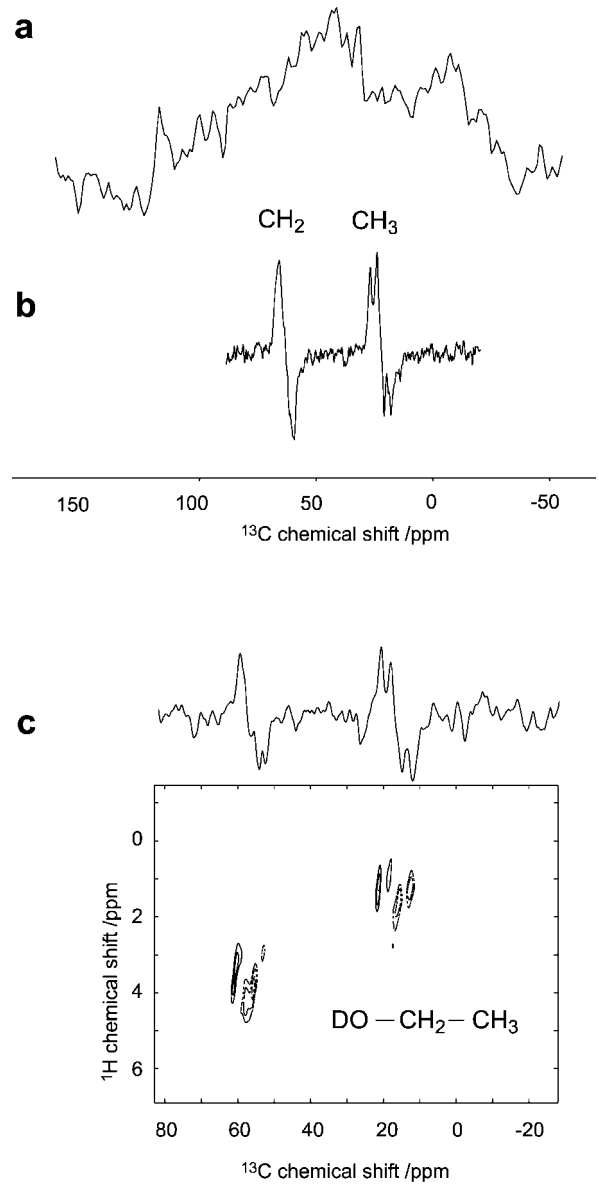

FIG. 6. (a) Single pulse ^{13}C NMR spectrum of ethanol-*d*1 (sample arrangement as in Fig. 3) in a B_0 field gradient of 0.4 mT/cm. (b) ^{13}C NMR spectrum of ethanol-*d*1 under the same conditions, obtained with pulse sequence of Fig. 2a. Nominal 90° pulse lengths were 9 and 11 μs for ^{1}H and ^{13}C, respectively, the β-pulse length was 8 μs at a dwell time of 200 μs, the delay $1/(2J)$ was set to 3.6 ms. (c) HETCOR spectrum of ethanol-*d*1 under the same conditions, obtained with the pulse sequence of Fig. 2b. The ratio k between the length of the t_1 time and the initial RF pulse in the proton dimension was 4.1.

arranged as shown in Ref. (*19*). A static B_0 field gradient of 0.4 mT/cm was applied. Figure 6a shows a single-pulse ^{13}C NMR spectrum of a sample of ethanol located outside of the coil, in the inhomogeneous B_0 field. The total linewidth due to the field gradient is 70 ppm, and the individual signals are not resolved. With the pulse sequence of Fig. 2a a resolved INEPT spectrum with one antiphase triplet $1:0:-1$ for the ^{13}C NMR-signal of the methylene group and one antiphase quartet $1:1:-1:-1$ of the methyl group of ethanol can be obtained as shown in Fig. 6b. Figure 6c shows a refocused HETCOR spectrum of ethanol, obtained under the same conditions with the pulse sequence of Fig. 2b. Both signals are clearly resolved in both dimensions, and the full phase information in the ^{13}C dimension is maintained.

CONCLUSIONS

We were able to extend the repertoire of nutation echo based pulse sequences for the observation of resolved NMR spectra in matched B_0 and RF field gradients toward high-resolution ex-situ 2D NMR. Two different types of nutation echoes in the indirect dimension were exploited for obtaining one-dimensional chemical shift images. The combination of an INEPT magnetization transfer step with a stroboscopic acquisition sequence produces resolved heteronuclear NMR spectra. Finally, we described a HETCOR sequence which yields heteronuclear correlations with high resolution in both dimensions. Although the experiments were performed inside the bore of a superconducting magnet with moderate field gradients, extensions of these pulse sequences may find application in external scanning spectrometers where they would be useful for ex-situ situations such as those existing in materials and biomedical application.

ACKNOWLEDGMENTS

This work was supported by the Director, Office of Science, Office of Basic Energy Sciences, Materials Sciences Division, of the U.S. Department of Energy under Contract DE-AC03-76SF00098. H.H. gratefully acknowledges the Alexander von Humboldt Foundation for support through a postdoctoral fellowship.

REFERENCES

1. R. L. Kleinberg, A. Sezginer, D. D. Griffin, and M. Fukuhara, Novel NMR apparatus for investigating an external sample, *J. Magn. Reson.* **97,** 466–485 (1992).
2. G. Eidmann, R. Savelsberg, P. Blümler, and B. Blümich, The NMR MOUSE, a mobile universal surface explorer, *J. Magn. Reson. A* **122,** 104–109 (1996).
3. M. D. Hürlimann and D. D. Griffin, Spin dynamics of Carr–Purcell–Meibohm–Gill-like sequences in grossly inhomogeneous B_0 and B_1 fields and application to NMR well logging, *J. Magn. Reson.* **143,** 120–135 (2000), doi:10.1006/jmre.1999.1967.
4. G. Zimmer, A. Guthausen, and B. Blümich, Characterization of cross-link density in technical elastomers by the NMR-MOUSE, *Solid State NMR* **12,** 183–190 (1998).
5. R. Haken and B. Blümich, Anisotropy in tendon investigated in vivo by a portable NMR scanner, the NMR-MOUSE, *J. Magn. Reson.* **144,** 195–199 (2000), doi:10.1006/jmre.2000.2040.
6. H. Y. Carr and E. M. Purcell, Effects of diffusion on free precession in nuclear magnetic resonance experiments, *Phys. Rev.* **94,** 630–638 (1954).
7. F. Balibanu, K. Hailu, R. Eymael, D. E. Demco, and B. Blümich, Nuclear magnetic resonance in inhomogeneous magnetic fields, *J. Magn. Reson.* **145,** 246–258 (2000), doi:10.1006/jmre.2000.2089.
8. A. Wiesmath, C. Filip, D. E. Demco, and B. Blümich, Double-quantum-filtered NMR signals in inhomogeneous magnetic fields, *J. Magn. Reson.* **149,** 258–263 (2001), doi:10.1006/jmre.2001.2299.
9. R. Kimmich, I. Ardelean, Y. Lin, S. Ahn, and W. S. Warren, Multiple spin echo generation by gradients of the radio-frequency amplitude: Two-dimensional nutation spectroscopy and multiple rotary echoes, *J. Chem. Phys.* **111,** 6501–6509 (1999).
10. I. Ardelean, R. Kimmich, and A. Klemm, The nutation spin echo and its use for localized NMR, *J. Magn. Reson.* **146,** 43–48 (2000), doi:10.1006/jmre.2000.2146.
11. P. H. Bolton and G. Bodenhausen, Resolution enhancement in heteronuclear two-dimensional spectroscopy by realignment of coherence transfer echoes, *J. Magn. Reson.* **46,** 306–318 (1982).
12. L. D. Hall and T. J. Norwood, Measurement of high-resolution NMR spectra in an inhomogeneous magnetic field, *J. Am. Chem. Soc.* **109,** 7579–7581 (1987).
13. M. Gochin, D. P. Weitekamp, and A. Pines, A SHARP method for high-resolution NMR of heteronuclear spin systems in inhomogeneous fields, *J. Magn. Reson.* **63,** 431–437 (1985).
14. D. P. Weitekamp, J. R. Garbow, J. B. Murdoch, and A. Pines, High-resolution NMR spectra in inhomogeneous magnetic fields: Application of total spin coherence transfer echoes, *J. Am. Chem. Soc.* **103,** 3579–3580 (1981).
15. J. R. Garbow, D. P. Weitekamp, and A. Pines, Total spin coherence transfer echo spectroscopy, *J. Chem. Phys.* **79,** 5301–5310 (1983).
16. J. J. Balbach, M. S. Conradi, D. P. Cistola, C. Tang, J. R. Garbow, and W. C. Hutton, High-resolution NMR in inhomogeneous fields, *Chem. Phys. Lett.* **277,** 367–374 (1997).
17. K. Nagayama, A. Kumar, K. Wüthrich, and R. R. Ernst, Experimental techniques of two-dimensional correlated spectroscopy, *J. Magn. Reson.* **40,** 321–334 (1980).
18. A. A. Maudsley, A. Wokaun, and R. R. Ernst, Coherence transfer echoes, *Chem. Phys. Lett.* **55,** 9–14 (1978).
19. C. A. Meriles, D. Sakellariou, H. Heise, A. Moulé, and A. Pines, Approach to high-resolution ex-situ NMR spectroscopy, *Science* **293,** 82–85 (2001).
20. A. Jerschow, Multiple echoes initiated by a single radiofrequency pulse in NMR, *Chem. Phys. Lett.* **296,** 466–470 (1998).
21. E. L. Hahn, Spin echoes, *Phys. Rev.* **80,** 580–594 (1950).
22. D. I. Hoult, Rotating frame zeugmatography, *J. Magn. Reson.* **33,** 183–197 (1979).
23. G. A. Morris and R. Freeman, Enhancement of nuclear magnetic resonance signals by polarization transfer, *J. Am. Chem. Soc.* **101,** 760–762 (1979).
24. R. Freeman and G. A. Morris, Experimental chemical shift correlation maps in nuclear magnetic resonance spectroscopy, *J. Chem. Soc. Chem. Commun.* 684–686 (1978).
25. S. Wimperis, Broadband, narrowband, and passband composite pulses for use in advanced NMR experiments, *J. Magn. Reson. A* **109,** 221–231 (1994).
26. A. A. Maudsley, S. K. Hilal, W. H. Perman, and H. E. Simon, Spatially resolved high resolution spectroscopy by "four-dimensional" NMR, *J. Magn. Reson.* **51,** 147–152 (1983).